10.3217/978-3-99161-093-9-016

Noninvasive self-paced BCI for lower limb exoskeleton control: a multi-session investigation of user learning

Alessio Lo Faro[1], Tommaso Cortecchia[2], Miroljub Mihalovic[1], Edoardo Trombin[1], Emanuele Menegatti[1,3], Luca Tonin[1,3], Stefano Tortora[1,3]

[1]Department of Information Engineering University of Padova, Padova, Italy
[2]Politecnico di Torino, Torino, Italy
[3]Padova Neuroscience Center, Padova, Italy

E-mail: stefano.tortora@unipd.it

ABSTRACT: Brain-Computer Interfaces (BCIs) represents a promising approach to incorporate the user's motion intention into the control of assistive technologies. However, its efficacy for the control of real lower-limb exoskeletons (LLE) remain largely overlooked, with most of the work in the literature focusing on single-session studies. To overcome these limitations, this work proposes and investigates the usage of a noninvasive electroencephalography (EEG)-based BCI for self-paced control of a LLE across multiple sessions. The proposed framework and training protocol are explicitly designed to promote progressive familiarization through repetitive training, continuous feedback, and minimal decoder calibration, encouraging the emergence of more stable and physiologically interpretable neural patterns. Experimental results show that all participants achieved functional LLE control within three sessions, paired with classification improvements and stabilization of cortical activation patterns. Overall, the findings support the feasibility of practical LLE-BCI systems while highlighting the importance of stable decoding strategies in online and multi-session experiments promoting user learning, which are key to achieving a more reliable and effective BCI-driven LLE control.

INTRODUCTION

In recent decades, the burden of motor disability resulting from neurological conditions has increased, mainly due to population aging and improved survival [1], resulting in an unmet need for new rehabilitation and assistive strategies. Lower-limb exoskeletons (LLEs) represent a promising assistive technology to compensate for motor impairments, enabling standing and walking capabilities that are otherwise impossible with conventional devices such as wheelchairs. Moreover, exoskeletons are increasingly considered as rehabilitation tools, as they allow intensive, repetitive, and task-oriented training with limited external assistance compared to traditional methods [2]. Nevertheless, current LLE are still characterized by unnatural control interfaces to translate user intentions into robot commands; in this context, Brain-Computer Interfaces (BCIs) enable a direct communication pathway between the brain and the external actuator. Therefore, the coupling of BCIs and exoskeletons has emerged as a promising approach both for motion substitution [3] and motor rehabilitation [4]. In particular, BCIs capturing the user's motion intention (MI) represent a natural solution for the control of limb prosthetics and exoskeletons without the need of overt movements or muscular activations [5]. While MI-based BCIs are well established for upper-limb exoskeleton control [6], the decoding of gait or feet MI presents intrinsic challenges: the cortical representation of the feet is deeper and more medial, resulting in weaker and less spatially distinct EEG features compared to upper-limb MI. These limitations have contributed to marked inter-subject variability, and a limited application for the control of real exoskeleton devices.

Among the challenges preventing the effective usage of BCI, non-stationarity of EEG signals and the high inter-session variability lead to requiring repeated calibrations of the BCI decoder [7]. To overcome these limitations, a new perspective, that has become recently popular, describes the BCI system not as a static decoder, but as a dynamic system composed of a learning user and an adaptive decoding algorithm [8]. Within this framework, performance gains may stem not only from more complex classification methods, but also from the user's increasing ability to produce stable and well-separated neural patterns through interaction with the system [9]. This view motivates training strategies that emphasize user learning and limit frequent decoder recalibration [10].

Within this context, the present work proposes a noninvasive EEG-based BCI system for the self-paced control

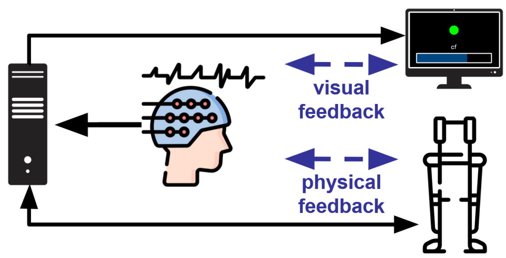

Figure 1: Experimental setup

10.3217/978-3-99161-093-9-016

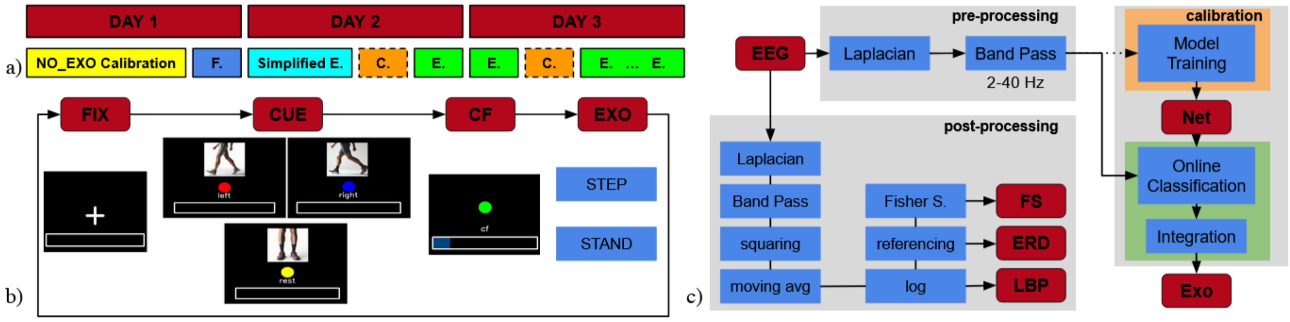

Figure 2: a) Sessions design: F: familiarization, C: calibration, E: evaluation. b) Experimental trial organization with the corresponding visual instructions. c) Data processing and classification pipelines.

of a LLE. Unlike existing studies, the proposed method specifically target the user learning, allowing the subjects to progressively familiarize with the BCI-LLE system, and improve their performance through closed-loop interactions with real-time neurofeedback. Analysis of multi-session performance and EEG features reveals that methodologies promoting user learning are critical for developing the stable, discriminant neural signatures necessary for effective LLE-BCI operation.

MATERIALS AND METHODS

Experimental setup: The experimental setup (shown in Fig. 1) consists of a 64-channel EEG acquisition system (Waveguard cap with eego64 aplifier, AntNeuro, Netherland) connected to a master PC running the software for data acquisition, processing, and classification. A monitor guided the experimental protocol and provided live feedback to the participant on the outcome of the BCI decoder. Physical feedback was provided by the open-source LLE ALICE (Interactive Technologies Studio INDI, France). During the experiments, all participants used hand crutches to maintain a correct and stable posture. The integration of all the different hardware and software components required for the experiment was achieved through ROS-Neuro [11], an extension of the Robot Operating System (ROS) for BCI applications.

Participants: Four healthy participants (3 male and 1 female) were recruited, with an age in the range of 23 to 25 years old. No participants had previous experience with BCI systems or LLE-assisted gait exercises. To identify them, an anonymous alphanumeric code was assigned to each participant: K9, L1, L2, L3.

Protocol and session design:
The protocol consists of a multi-session experiment organized in three different days, as shown in Fig. 2a. Based on the session, the protocol is organized in five different phases for user familiarization, decoder calibration, and online evaluation. During familiarization, participants interacted with the LLE without EEG acquisition, and an external operator triggered the command for the exoskeleton. The calibration phases involved EEG acquisition during visually guided MI of left or right stepping (Movement class) or relaxation (Rest class), organized in runs of 16 trials. The organization of each trial is shown in Fig. 2b, and includes a 2-second fixation period, a 2-second task cue, and a continuous feedback phase (4 s for Movement classes, 8 s for Rest), during which participants performed the instructed mental task.Only in the first day, calibration runs are performed without the exoskeleton and with the subject straight standing in front of the monitor (No-Exoskeleton Calibration). These data are used to calibrate the first subject-specific decoder. In the online evaluation phases, the classifier outputs are processed in real time and used to control the visual feedback. The evaluation runs consist of 16 trials where movement is discriminated from rest, with the same organization as in Fig. 2b. Due to the difficulty in reliably distinguishing left from right feet imagery [12], movement classes were merged during classification, also motivated by the natural alternation of left-right steps in gait. At trial completion, the exoskeleton executed the cued movement to provide physical feedback. A simplified evaluation protocol was also introduced in early online testing and bias inspection, providing exclusively positive feedback by responding only to correct classifier outputs. Following the first calibration, we maintained the same decoding model for each subject also in the following days whenever possible. New calibration runs with the subjects wearing the exoskeleton and a decoder retraining (either a complete recalibration or a fine tuning of the existing model) were performed if the recognition rate of a class dropped below 55% in two consecutive runs. Each session lasted less than two hours, including setup preparation, user instruction, and experimental execution, to minimize fatigue and habituation. At least 8 evaluation runs per subject were acquired to ensure a sufficiently large evaluation dataset.

Data analysis: Two independent pipelines were ideated as shown in Fig. 2c: one to prepare the dataset for the online decoders, and a second pipeline for the analysis of the neural features and user learning. EEG signals are sampled at 512 Hz and processed using a 1 s sliding window shifted every 62.5 ms (frame rate of 16 Hz). Thirty-two central electrodes around Cz were selected from the 64-channel montage according to the international 10–10 system (frontal to parietal sites); AFz and CPz were used as ground and reference, respectively.

10.3217/978-3-99161-093-9-016

For the online experiments the signals were firstly filtered by a spatial Laplacian operator. Subsequently a 5th-order Butterworth bandpass filter with cut-off frequencies set at 2 and 40 Hz was employed. Offline, the EEG signals were transformed into a set of spatial–spectral features. Log-band power (LBP) was computed in the $\delta - \theta$(1–8 Hz), μ(8–13 Hz), and β(13–32 Hz) bands using band-pass filtering, signal squaring, moving-averaging, and logarithmic scaling. Temporal modulations were quantified via event-related desynchronization/synchronization (ERD/ERS) utilizing the signal recorded during the fixation period as the reference. Feature discriminability between rest and movement tasks was assessed using the Fisher's Score (FS), yielding discriminant features maps across electrodes and frequency bands.

Classification: For each subject, three deep learning models were selected and trained individually on the pre-processed calibration data: EEGNet [13]; PhiNet [14], and a Temporal Graph Convolutional Network [15].
For online evaluation, the model yielding the best validation performance on the calibration data was selected. To improve the robustness of the system against single-sample classification noise, classifier outputs $C_i(t)$ were integrated over time at 16 Hz as follow: $v_i(t) = v_i(t-1) + (C_i(t) - 0.5)/ev$. The integrated values v_i are clipped to the [0, 1] interval, therefore in our two-class configuration, v_{Rest} and $v_{Movemet}$ remain symmetric around 0.5. For controlling the exoskeleton, the overall decision was treated as a one class problem: rest state is maintained until $v_{Movement}$ (represented by the bar on the visual feedback) reached a threshold th, triggering therefore a step command and ending the trial. Dynamics were governed by tuning the confidence threshold th and the ev evidence-velocity accumulation parameter, allowing control over system's sensitivity.

Evaluation metrics: System performance was evaluated using both standard classification metrics and a task-specific temporal measure. Classification accuracy and F1 score were computed to assess single-sample and trial-level discrimination performance. In addition, a normalized time score [9] was used to quantify the trade-off between system reactivity to MI and robustness against false activations during rest.

$$normTimeScore = \frac{(timeout - \hat{T}_{Rest}) * n_{rest} + \hat{T}_{Mov} * n_{Mov}}{timeout * 2 * n_{tot}} \tag{1}$$

$\hat{T}_i$ is the mean time required to complete the task of the i^{th} class and n_i is the total number of task performed; therefore, lower values indicate a faster and more reliable system. The *timeout* is set at 10 seconds as it is the maximal duration of the continuous feedback for the rest trials.

RESULTS

Feature analysis: For all the participants, a total of 10 calibration runs per subject were acquired in different days and used to analyze the evolution of the discriminant features over time in the $\delta - \theta$, μ and β bands. The

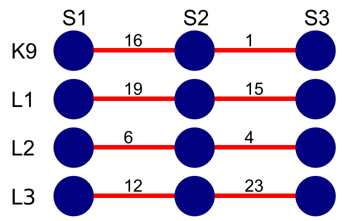

Figure 3: interval (in days) between two consecutive sessions.

interval in days between two consecutive sessions is reported in Fig. 3, while Fig. 4 reports the FS maps for each calibration run calculated on the β band. To assess the stability of the generated neural patterns over time, Fig. 4 shows the euclidean distances between the FS distributions of consecutive runs, measuring the similarity between the discriminant features used for MI classification [10]. This analysis was performed for each frequency bands. To enable inter-subject comparison, vectors were normalized by the mean norm of subject-specific FS vectors. Interestingly, all the subjects show a statistically significant decrease of the between-run distance throughout the experiment, particularly in the μ and β bands, highlighting an increase in the temporal consistency of the neural features in these bands.

Classification models: For each participant, the adopted policy aimed to maintain the same classifier for as long as possible. To analyze the decoding stability for the LLE control, Fig. 5 illustrates, for each session and participant, whether it was necessary to train a new classifier, perform a fine-tuning of the existing model with the new data, or whether the classifier was preserved as it was. Additionally, the preferred model for each subject is also reported. All the subjects required a full model recalibration at the beginning of the second session, while the previous model was preserved in the third session with a model fine-tuning for subjects L1, L2 and L3.
Online evaluation results: Fig. 6 reports the evolution of the performance metrics over time, showing an overall increase of performance with training for all the subjects. To analyze the adjustments of the control dynamic, Tab 1 reports the values of the hyperparameter ev and threshold th used during each evaluation run. Finally, to provide a qualitative perspective of the evolution of the system performance, Fig. 7 reports the single-trial results obtained during the first and last runs of the two evaluation sessions. Green lines correspond to successful trials, while red lines to failures.

DISCUSSION

Features analysis: The evolution of the FS spatial distributions suggests a progressive consolidation of discriminant neural patterns across sessions. Despite inter-subject variability, all participants exhibit increasing centralization of discriminant features in at least one frequency band, mainly along midline sensorimotor regions. This behavior supports the hypothesis that repeated inter-

 10.3217/978-3-99161-093-9-016

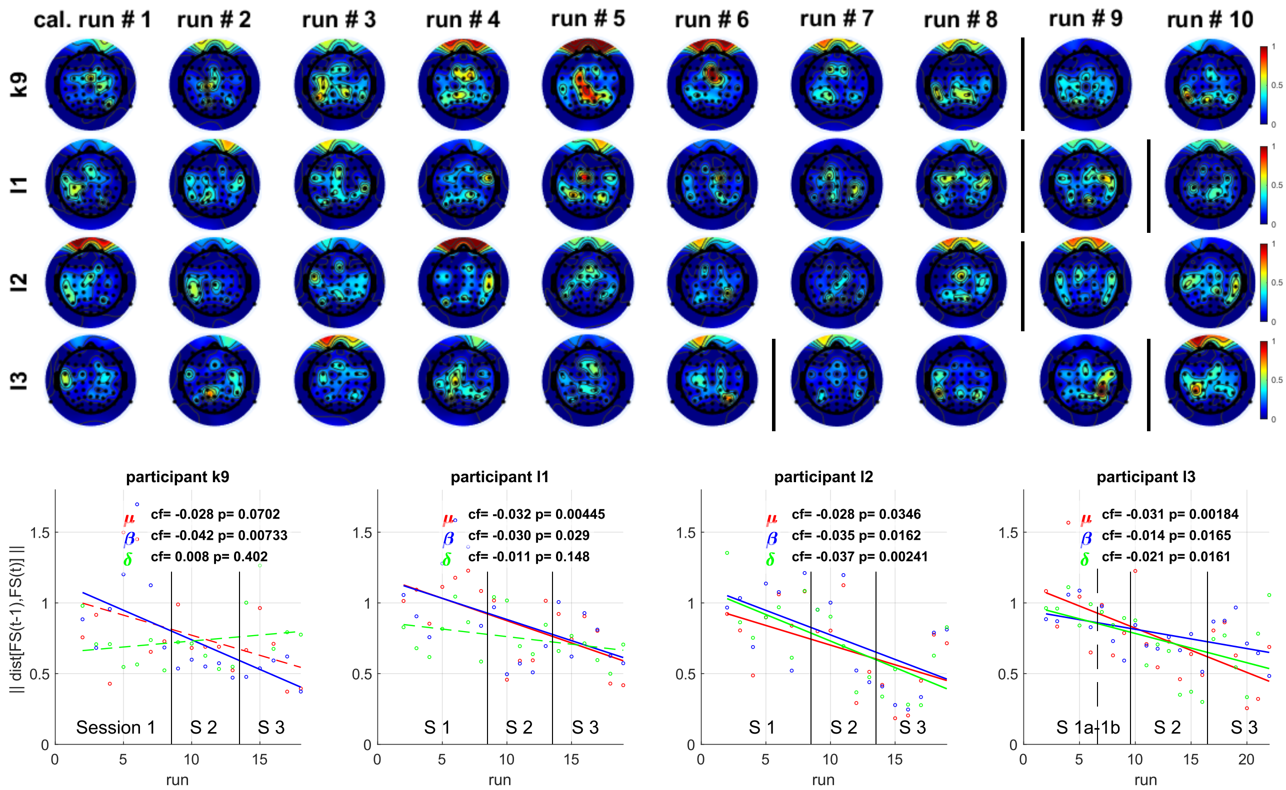

Figure 4: (Top) Features maps computed in the β frequency band for each calibration run; vertical lines correspond to the start of a new session. (Bottom) Normalized between-run FS distances across runs for each participant and frequency band. Correlation calculated using Spearman correlation test (full line when significant, i.e., p < 0.05 two-tiled t-test, dashed line otherwise).

participant	S2 start	S2 end	S3 start	S3 end
K9	TGCN	TGCN	TGCN	TGCN
L1	EEGNet	EEGNet	EEGNet	EEGNet
L2	PhiNet	PhiNet	PhiNet	PhiNet
L3	PhiNet	PhiNet	PhiNet	PhiNet

complete recalibration
fine tuning
no recalibration

Figure 5: Classifier updates before or during each evaluation sessions.

Table 1: Hyperparameter values during online evaluation runs

	K9		L1		L2		L3	
	ev	th	ev	th	ev	th	ev	th
run 1 S2	56	0.8	48	0.7	48	0.7	56	0.7
run 2 S2	48	0.8	48	0.8	48	0.7	48	0.6
run 3 S2	48	0.8	48	0.8	56	0.8	48	0.7
run 4 S2	48	0.8	48	0.8	–	–	48	0.65
run 5 S2	–	–	–	–	–	–	48	0.65
run 6 S2	–	–	–	–	–	–	48	0.65
run 1 S3	48	0.8	56	0.8	48	0.75	48	0.8
run 2 S3	48	0.8	56	0.8	48	0.8	48	0.7
run 3 S3	48	0.8	48	0.8	48	0.85	48	0.75
run 4 S3	48	0.8	48	0.8	56	0.8	56	0.8
run 5 S3	–	–	48	0.8	56	0.85	56	0.7
run 6 S3	–	–	–	–	56	0.8	–	–

action with the BCI promotes user-driven neural adaptation. Among the analyzed bands, the β rhythm shows the most consistent involvement across participants, combining high discriminative power with a gradual alignment of spatial hot spots toward centrally located electrodes. Although complete spatial stabilization is not achieved, the concurrent steady decrease in run-to-run variability of FS vectors indicates increasing stability of cortical activation patterns. The $\delta - \theta$ band exhibits weaker and less consistent trends, which may be related to its involvement in movement-related neural processes, as suggested by studies focusing on locomotion decoding [16]. On the other hand, the major effect is visible in the μ and β bands Since for the subjects the novelty lies in the mental exercise, and not in the performance of a complete gait cycle, it would therefore seem reasonable that the most evident improvements occur in the μ and β sensory motor rhythms (SMR), suggesting an emergence of more stable and discriminant movement-related features consistent with existing literature on motor learning and cortical plasticity [17].

Online evaluation results: When performance metrics are aggregated across subjects, a general tendency toward improved classification accuracy over time emerges, although the magnitude and statistical robustness of these effects vary across individuals. Most participants exhibit significant increases in trial- or sample-level accuracy, while one subject shows no clear performance trend, confirming the pronounced inter-subject variability typical of MI-based BCI systems [8, 10]. Across sessions, the normalized time score decreases, particularly for participants showing trial accuracy improvements. This concurrent evolution suggests that performance gains are not merely the result of integrator tuning, but reflect a genuine performance improvement. From an individual perspective, participant K9 demonstrates the most consistent learning behavior, with significant improvements in

10.3217/978-3-99161-093-9-016

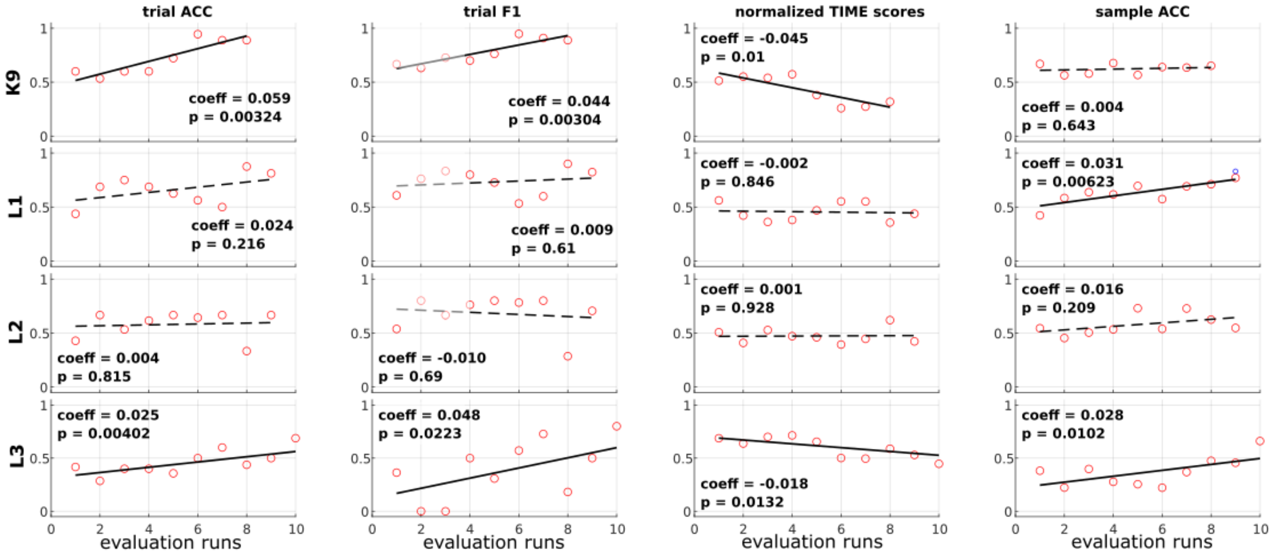

Figure 6: Performance metrics across the evaluation runs for each participant. Correlation calculated using Spearman correlation test (full line when significant, i.e., p < 0.05 two-tiled t-test, dashed line otherwise).

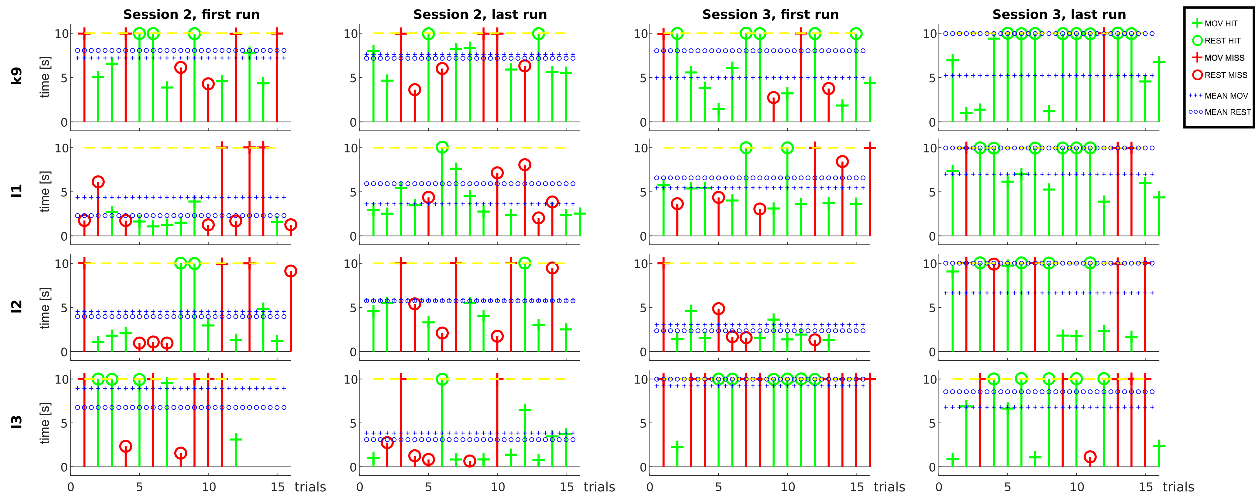

Figure 7: Single trial outcomes of online evaluation runs. For each evaluation session the first and the last run are considered. Green labeled stems represent a positive outcome while red stem correspond to failed attempts.

trial-level metrics and response efficiency despite minimal parameter adjustments and no decoder recalibration. L1 and L3 participants exhibit milder but steady statistically significant improvements, while L2 shows the lowest improvements, even if with classification accuracies always above chance level. Despite this, after classifier updates and hyperparameters tuning processes, also L2 showed some improvements in the control of the LLE at the end of the experiment, as visible in Fig. 7, similar to the other participants. These observations emphasize the need for subject-specific strategies to accommodate heterogeneous learning and control capabilities. Overall, the results support the interpretation that even a limited number of training sessions can induce measurable user adaptation, contributing to system-level performance improvements. In particular, the dissociation observed between single-sample and trial-based accuracy in some participants suggests that learning may manifest as increased temporal stability of neural patterns, rather than as instantaneous classification gains, reinforcing the role of user learning in effective BCI control.

CONCLUSION

The experimental results obtained confirm that the proposed protocol based on repeated sessions, continuous feedback, and limited calibration is capable of supporting the development of a functional LLE-BCI system while simultaneously promoting neural learning processes in the user. The analysis of feature maps reveals a progressive centralization of discriminant information in midline channels toward physiologically meaningful frequency bands (μ and β) over the course of the sessions. This suggests that cortical adaptation occurs associated with

 10.3217/978-3-99161-093-9-016

the user's familiarization with the motor imagery task. Although the ERD/ERS represent a simplified characterization of the EEG input compared to the internal representations of deep networks, they are widely used in the literature to interpret task-related dynamics, and still provide meaningful insight into subject-specific improvements. In parallel, improvements in reaction times and an increase in online test accuracy metrics further support the hypothesis that the protocol promotes genuine BCI learning. At the same time, the results highlight the need for a dynamic evolution of classification methodologies capable of adapting to individual peculiarities.

With appropriate training of the user and a shared control policy with the robot, this approach could support continuous lower-limb exoskeleton control driven by motor intention and not constrained by predefined cues; however, this requires highly reliable classification of the rest state, particularly in complex environments.

Limitations and future developments: Although the study achieved positive results, some limitations must be acknowledged. First, the participant cohort is relatively small and does not allow population-level analyzes: larger studies would be required to explore whether individual factors influence the modulation of right/left step imagination. Secondly, additional sessions could have provided a clearer assessment of user adaptation over time and allowed the evaluation of the stability of the observed results across sessions, which is currently visible at the end of the third sessions. Another relevant limitation concerns the use of healthy volunteers, as this choice may introduce a translation gap [5]. Future validation on motor-impaired end users will be necessary to assess the clinical applicability of the proposed framework.

Finally, although the framework allows the acquisition of lateralized stepping data, classifiers were trained to decode a generic stepping command. This design choice enabled robust control for novice users, but precluded the evaluation of left–right motion intention discrimination. Future work may investigate lateralized decoding after extended training.

ACKNOWLEDGMENT

This work was funded by Next Generation EU - “Age-It - Ageing well in an ageing society” project (PE0000015), NRRP - PE8.

REFERENCES

[1] GBD 2021 Nervous System Disorders Collaborators. Global, regional, and national burden of disorders affecting the nervous system, 1990–2021: A systematic analysis for the Global Burden of Disease Study 2021. Lancet Neurol.. 2024;23(4):344–381.

[2] Hsu TH, Tsai CL, Chi JY, Hsu CY, Lin YN. Effect of wearable exoskeleton on post-stroke gait: A systematic review and meta-analysis. Annals of Physical and Rehabilitation Medicine. 2023;66(1):101674.

[3] Hramov AE, Maksimenko VA, Pisarchik AN. Physical principles of brain–computer interfaces and their applications for rehabilitation, robotics and control of human brain states. Physics Reports. 2021;918:1–133.

[4] Frolov AA et al. Post-stroke rehabilitation training with a motor-imagery-based brain-computer interface (bci)-controlled hand exoskeleton: A randomized controlled multicenter trial. Frontiers in Neuroscience. 2017;11:400.

[5] Tonin L, Millán JdR. Noninvasive brain–machine interfaces for robotic devices. Annual Review of Control, Robotics, and Autonomous Systems. 2021;4:191–214.

[6] Khan MA, Das R, Iversen HK, Puthusserypady S. Review on motor imagery based bci systems for upper limb post-stroke neurorehabilitation: From designing to application. Computers in Biology and Medicine. 2020;123:103843.

[7] Saha S, Baumert M. Intra-and inter-subject variability in eeg-based sensorimotor brain computer interface: A review. Frontiers in computational neuroscience. 2020;13:87.

[8] Perdikis S, Tonin L, Millán JdR. Brain-machine interfaces: A tale of two learners. IEEE Systems, Man, and Cybernetics Magazine. 2020;6(2):32–42.

[9] Ceradini M, Tortora S, Micera S, Tonin L. The effect of user learning for online eeg decoding of upper-limb movement intention. IEEE Transactions on Medical Robotics and Bionics. 2025;7(2):633–641.

[10] Tortora S et al. Neural correlates of user learning during long-term bci training for the cybathlon competition. Journal of NeuroEngineering and Rehabilitation. 2022;19:69.

[11] Tonin L, Beraldo G, Tortora S, Menegatti E. Rosneuro: An open-source platform for neurorobotics. Frontiers in Neurorobotics. 2022;16:886050.

[12] Tariq M, Trivailo PM, Simic M. Eeg-based bci control schemes for lower-limb assistive-robots. Frontiers in human neuroscience. 2018;12:312.

[13] Lawhern VJ, Solon AJ, Waytowich NR, Gordon SM, Hung CP, Lance BJ. Eegnet: A compact convolutional neural network for eeg-based brain–computer interfaces. Journal of Neural Engineering. 2018;15(5):056013.

[14] Ishikawa S, Yamada M, Bao H, Takezawa Y. Phinets: Brain-inspired non-contrastive learning based on temporal prediction hypothesis. In: International Conference on Representation Learning. 2025, 68386–68412.

[15] Hou Y et al. Gcns-net: A graph convolutional neural network approach for decoding time-resolved eeg motor imagery signals. IEEE Transactions on Neural Networks and Learning Systems. 2022;35(6):7312–7323.

[16] Tortora S et al. Effect of lower limb exoskeleton on the modulation of neural activity and gait classification. IEEE Transactions on Neural Systems and Rehabilitation Engineering. 2023;31:2988–3003.

[17] Espenhahn S et al. Sensorimotor cortex beta oscillations reflect motor skill learning ability after stroke. Brain Communications. 2020;2(2):fcaa161.